Effect of highly efficient steam explosion treatment on beech, poplar and spruce solid wood physicochemical and permeable performances

He Qian, Qianqian Hou, Lu Hong, Xiaoning Lu, Isabelle Ziegler-Devin, Laurent Chrusciel, Arnaud Besserer, Nicolas Brosse

Effect of highly efficient steam explosion treatment on beech, poplar and spruce solid wood physicochemical and permeable performances.1[1]

Qian HE[1,2,3], Qianqian Hou[1], Lu Hong[4], Xiaoning Lu[3], Isabelle Ziegler-Devin[2], Laurent Chrusciel[2], Arnaud Besserer[2], Nicolas Brosse[2]*

[1]College of Civil Science and Engineering, Yangzhou University, Yangzhou 225127, P. R. China

[2]Université de Lorraine, INRAE, LERMAB, GP4W, F-54000 Nancy, France

[3]College of Materials Science and Engineering, Nanjing Forestry University, Nanjing, 210037, P.R. China

[4]College of Forestry and Landscape, Anhui Agricultural University, Hefei, 230036, P.R. China

*Corresponding author: Nicolas Brosse

Email address: Nicolas.Brosse@univ-lorraine.fr

Abstract:

The effect of steam explosion treatment (SE) on the appearance and water permeability of solid beech, poplar, and spruce wood was investigated. Wooden test specimens were steam blasted after water or acid impregnation at 10 ~ 16 bar for 5 ~ 15 minutes, and their chemical composition was determined by chromatographic analysis after hydrolysis and infrared spectroscopy. Macro/micro cracks with shrinkage and reduced sphericity after drying were observed by scanning electron microscopy. Darker color and more severe changes in colorimetric parameters were measured spectrophotometrically for SE treated samples, especially under acidic conditions or higher severity factors (SF). To some extent, the physicochemical and permeability properties of SE treated wood samples could be simulated by considering the correlations of the different factors. No significant deterioration in chemical content, longitudinal compressive modulus of elasticity ($MOE_{//}$) and modulus of rupture ($MOR_{//}$) was observed in SE specimens treated with water. Higher permeability was obtained under a mild condition of 180°C-5 min for poplar and a higher SF condition for beech and spruce. Therefore, SE could be an efficient method for modifying solid wood to improve its permeability and functionality.

Keywords: steam explosion, solid wood, morphology, color, chemical changes, compression, permeability

1. Introduction

An increasing interest is given to wood material because of its renewable, ecological and inexpensive characteristics (Souza et al., 2018; Akpan et al., 2021). However, due to the composition of the cell wall of wood, which consists of cellulose, hemicellulose, and lignin, some disadvantages have been identified, including rotting and poor fire resistance indoors and outdoors (Can et al., 2019). Different types of preservatives or flame retardants have been used to modify the wood to obtain a high-performance material (Zelinka et al., 2019; Pondelak et al., 2021). Marco/micro-porous structures provide an opportunity for these functional reagents to penetrate the wood by impregnation (Taghiyari et al., 2021). Macroscopic pores in tracheids or vessels are the main penetration channels in the longitudinal direction of the wood while pits and rays are the microscopic pores connecting the transverse channels between tracheids or vessels (Tarmian et al., 2020). However, some of chemical constituents such as extracts or thylose and the structure of the aspirated pits in the wood have a negative influence on the wood penetrability (Monteiro et al., 2020; Zhang and Cai, 2009).

Many physicochemical methods have been used in the pretreatment of wood to improve its penetrability. It has been shown in previous studies that acidic, alkaline and organic or inorganic reagents can allow the formation of microscopic pores and flow channels in the anatomical structure of wood while causing the degradation of chemical contents such as hemicellulose, lignin and extracts (Nicholas, 1977; Stamm, 1932; Qu et al., 2021). Humar et al. have investigated the effect of swelling agents

including triethanolamine and formic acid on the penetration of copper-ethanolamine based preservatives into wood and significant improvement of permeability of preservatives was observed with negatively affecting their high leachability (Humar et al., 2011). James et al. demonstrated that the permeability of alkali-treated wood chips was greatly increased by saponification of the esters and the weakening of the intercellular region of the wood structure (Minor and Springer, 1993). Xu et al. explored the influence of supercritical carbon dioxide (SC-CO_2) on the permeability of hardwood and found highly improved penetration efficiency due to the reduction of tyloses involved in the vessels (Xu et al., 2019).

Physical methods such as ultrasonic, cryogenic freezing and hydrothermal treatments have also been widely utilized to improve wood permeability as well (Tanaka et al., 2010; Yorur and Kayahan, 2018). Hydrothermal treatments play a significant role in the improvement of permeability and the appearance of wood, attributing to the degradation of hemi-cellulose and polysaccharide decomposition under the release of acetic acid and other substances (Esteves et al., 2008). Steam explosion (SE) treatment is one of the specific hydrothermal treatments and has been applied in biomass modification, which is characterized by its facility, high efficiency and environmental friendliness (He et al., 2020). The lignocellulosic material is subjected to steam at high temperature and pressure for a certain period of time, and then the pressure is suddenly released (Martino et al., 2017; Donaldson et al., 1988). In general, studies have focused almost exclusively on fractionated wood (sawdust and chips) in order to increase the accessibility of cellulose to biocatalysts. Seidel et al.

has investigated the enzymatic digestibility of different biomasses under SE treatment and a positive influence on the enzymatic digestibility of softwood and hardwood species was observed, especially with high enzyme dosage (Seidel et al., 2017). Balan et al. studied the most desired conditions of the enzymatic hydrolysis reaction in order to optimize the pretreatment for a certain biomass (Balan et al.,2020). Simangunsong et al. have investigated the effect of particle size and severity factors on the xylan recovery of beech wood under SE treatment and the high degradation extent of hemicellulose was obtained for the smallest particle size of biomass with incomplete autohydrolysis at the largest particle sizes (Simangunsong et al., 2020).

In the literature, very little work has been done on the steam explosion of solid wood and the morphological impact of the process on the structure of the wood. Some works described an increase in the permeability of solid exploded wood by steam explosion but at low pressure (2~7 bars). It has been shown that low pressure SE treatment can induce an extension on lumina volume, a destruction on the obstacles and aspirated pits among wood structure, leading to the increase of wood permeability (Kanagaw, 1992). Kang et al. explored the effect of SE at low pressure on wood cell walls and higher permeability with the observation of better sound absorption coefficient (Kang et al., 2021). Kang et al. also discussed the effects of SE treatment on the appearance, anatomical features, permeability and sound absorption capability (SAC) of yellow poplar with improvement in permeability and SAC along the grain direction. Muzamal et al. (2017) described the formation of microcracks in wood cell walls following actual steam explosion of softwood (14 bars, 10 min). They showed

that the largest deformations and damages in the radial cell wall were observed in earlywood cells (Muzamal et al., 2017).

Therefore, a better understanding of the phenomena induced by SE on the macro/micro-morphology, the redistribution of chemical contents and the physical properties of wood seems therefore important for future applications. However, the physicochemical and permeable properties of SE treated solid wood has not been investigated in detail.

In this study, three solid wood species were selected including spruce, poplar and beech in order to investigate the physicochemical and permeable properties of SE treated solid wood. The color difference parameters, macro-graphs, anatomical features, mass loss, pH value of liquid phase, chemical contents, FTIR measurement mechanical properties, and impregnation rate were explored for solid wood samples under varied severity factors (SF) of SE treatment. The comparison of physicochemical and permeability characteristics of SE-treated solid wood was conducted among different species and varied SFs of SE treatments.

2. Materials and methods

2.1 Solid wood material

Spruce (*Picea glauca*), poplar (*Populus alba*) and beech (*Fagus sylvatica*) wood species harvested in Frace were used in this study. The density of the wood species was 0.43, 0.46 and 0.70 g/cm^3, respectively and the dimension of the wood samples were 200 mm (longitudinal) × 20 mm (radial) × 20 mm (tangential). None visible defects and decay were found for solid wood samples. Then, they were half cut to the

dimension of 100 mm (longitudinal)× 20 mm (radial)× 20 mm (tangential) and half of them were reserved as the controls. All the specimens were oven-dried at 103°C for 24h to achieve absolute dry mass.

2.2 Steam explosion (SE) treatment

The specimens were immersed in the distilled water or 1% H_2SO_4 (dilute sulfuric acid, by vol.) for 15 h at 25°C under vacuum condition and the pressure was released every 15 min (-0.09 MPa). After immersion, all the specimens were drained off and put into the reactor of SE equipment. Four kinds of severity factors (SFs) of SE treatment were selected as shown in **Table 1** (Vroom, 1957; He et al., 2020). After SE treatment, the liquid phase was collected and treated solid wood specimens were oven-dried at 103°C for 24h to achieve absolute dry mass. Eight repetitions were conducted for each condition.

Some details for the SE treatment: The main equipment involved in SE treatment included a steam generator, a high-pressure reactor (the volume of the reactor is 4L) and a discharge tank to receive the specimens after SE explosion. During the SE process, the saturated steam with high pressure was prepared by the steam generator. Then, the steam went continuously into the high-pressure reactor with the wood specimens in it for a duration. The wood specimens were put into the reactor in advance. After that, a sudden pressure drop (300 ms) occurred and the vapor expanded into the wood specimens. Finally, the treated specimens went into the discharge tank (Simangunsong et al., 2020; Ziegler-Devin et al., 2021).

2.3 Mass loss and pH measurement

The mass loss was tested according to the equation (1) based on the mass of dried solid wood specimens before and after SE treatment. pH value of liquid phase was measured by an acid-base testing device (PH-25/3C, Want Balance Instrument Co., Ltd., P.R.China). Three repetitions were conducted for each condition.

$$\text{Mass loss (\%)}=(\text{mass}_{\text{untreated}}-\text{mass}_{\text{treated}})/\text{mass}_{\text{untreated}}\times 100\%] \quad (1)$$

2.4 Color difference

The parameters of surface color difference for solid wood specimens were measured by a spectrophotometer (CM-600d, Konica Minolta Co. Ltd., Japan). ΔL^*, Δa^*, Δb^* and ΔE are the intensity of brightness to darkness, greenness to redness, blueness to yellowness and the total color difference, respectively. The parameters were recorded and compared between the control and treated specimens. The methodology of colour difference calculation was listed in the supplementary material.

2.5 Chemical contents measurement

Free extracts of milled wood powder (1g, 60 mesh) prepared from the control and treated specimens were utilized to test the contents of acid-insoluble lignin and monomeric sugars based on TAPPI T222 om-02 and NREL/TP-510-42618~c42622 standard by high-performance liquid chromatography (HPLC, ICS-3000 Dionex).

2.6 ATR-FTIR spectra

Milled wood powder (60 mesh) prepared from the control and treated specimens was measured by a Fourier transform infrared device (NICOLET 6700). The recording range was from 400 to 4000 cm^{-1} and the resolution for the device is 4 cm^{-1}.

2.7 Micro-structure measurement

The scanning electron microscope was used to observe micro-structure of solid wood specimens (TM-1000, Hitachi, Japan). The gold layer was deposited on the wood surface under vacuum condition prior to the observation. The sphericity for the shapes of lumina (or tracheids) and wood fiber cells was calculated by Matlab with the comparison of the circle shape (value = 1). The methodology of sphericity calculation was listed in the supplementary material.

2.8 Mechanical measurement

The longitudinal compression modulus of elasticity and modulus of rupture (parallel to the grain, $MOE_{//}$ and $MOR_{//}$) were measured by a universal testing machine according to the standard ASTM D4761-05. The dimension of specimens was 60 mm (longitudinal) × 20 mm (radial) × 20 mm (tangential). The specimens after SE treatment were oven-dried at 103°C for 24h to achieve absolute dry mass and they were sealed in the plastic bags for two weeks in the lab (20°C/65%RH) before the mechanical measurement. The loading speed was 2mm/min and the failure was achieved in 1min. Three repetitions were conducted for each condition.

2.9 Impregnation rate measurement

The control and treated solid wood specimens were put into an impregnation tank. After closing the tank, the air was pumped out under a pressure of -0.09 MPa for 30min. Then, water was pumped into the tank under a pressure of 10 bar for 20 min. After impregnation, all the specimens were put out and drained off. The change ratios of mass before and after impregnation were measured for all the specimens according to the equation (2). Three repetitions were conducted for each condition.

$$[\text{Impregnation ratio } (\%)=(\text{mass}_{\text{after}}-\text{mass}_{\text{before}})/\text{mass}_{\text{before}}\times 100\%] \quad (2)$$

Where $\text{Mass}_{\text{before}}$ representing the mass for dried samples and $\text{mass}_{\text{after}}$ representing the mass of samples after impregnation process.

3. Results and discussions

Wooden test specimens (100 mm × 20 mm × 20 mm) have been steam-exploded after water or acid impregnation according to the procedure described in section 2.2 and in **Table 1**.

3.1 Macro-/micro-morphology properties

The graphs of macro-morphology for solid wood specimens before and after SE and their color differences are shown in **Figure 1**. Darken color was observed for the treated specimens, especially for the higher SF or for the acidic conditions. The color difference parameters were further measured and calculated (**Figure 2**). For beech, poplar and spruce specimens, higher change ratios were observed for ΔL and ΔE compared with other parameters. ΔL highly decreased while the total color difference of ΔE increased after SE treatment. The highest change ratios (ΔL, ΔE, Δa and Δb) were observed for the acid treatment because of hydrolytic and oxidative coloring reactions among wood components during SE treatment (Sikora et al., 2018). As stated in previous studies, degradation of cell wall components occurred during the thermal treatment, leading to deacetylation of hemicelluloses, modification of lignin network and production of chromophores (Sundqvist, 2002; Nimz, 1984). As a result, oxidation and hydrolysis products such as quinones, acetic acid and other substances are the main reason for the color variation under hydrothermal process. In addition, it

was observed that the degree of darkening of the wood surface depended on the wood species. For the SE-treated specimens with distilled water immersion, significant liner relationship between SF and color difference parameters (ΔL and ΔE) was found for each wood species with high correlation coefficient of more than 90% (**Figure 2d and 2e**).

Some cracks were also observed in the cross-section of the hardwood specimens as shown in **Figure 1**. These cracks, which resembled honeycombs, occurred mainly along the rays of the wood. As investigated in previous studies, wood rays presented maximum tensile stress during the initial drying stage. Then, cracks appeared and spread in the radial direction, frequently between or along the rays, associated with wavy folds on the wood surface. These cracks which increased with the duration of SE treatment were attributed to high moisture content involved during the cooking phase of SE and to high temperature used in the drying process (Oltean et al., 2007; Simpson, 1991). The softwood displayed a different behavior as seen in **Figure 1c**. The spruce specimens have a highly modified surface and wood bundles were obtained after pressure release of SE treatment. This result was attributed to the different anatomical characteristic, chemical components and macropolymers involved in different wood species. Beech and poplar mainly consisted of wood fiber cells and lumen, which play a significant role in the resisting to the impact. While, spruce mainly consisted of the tracheids structure and the stress concentration could affect the whole structure during the impact.

The micro-structure was investigated as well for different wood specimens and

compared with the control as shown in **Figure 3, Figure S1, S2 and S3**. For the control, the specimens show morphology consistent with hardwood (**Figure 3a and 3b**) or softwood (**Figure 3c**) respectively. For beech, poplar and spruce specimens (**Figure S1a, S2a andc S3a**), the spiral thickening and pits structure were completely involved in smooth cell walls from longitudinal direction. Besides, the scalariform perforation plates between the vessels were naturally long with many partitions. Some local cracks were observed from both sections as well and these could be attributed to the samples preparation (Bekhta et al., 2016).

After SE treatment, in cross section visible deformations and axial cracks were observed for vessels or tracheids. For beech, poplar and spruce, some fibers, vessels and tracheids shranked considerably and the deformations were uneven, accompanied by an obvious reduction in lumen size especially for the condition of 180°C and 15 min (**Figure 3**). The shapes displayed in different colors of lumen (or tracheid) and wood fiber cell were selected from the micrographs of the control and SE-treated specimens. The sphericity for these shapes was calculated based on the circle shape and the correlation between the SF and sphericity for different wood species was as shown in **Figure 4**. Significant decrease of sphericity was obtained for the treated specimens compared with the control, especially with the higher SF=3.53 (180°C and 15 min) for hardwoods and SF=3.64 for spruce. Besides, the lowest sphericity was achieved for the treated poplar sample under the condition of SF=3.53 as indicated in **Figure 3b**. Nonlinear correlation of the SF and sphericity of cellular structure was observed for spruce specimens with the correlation coefficent of 85.98% while no

significant relationship was for beech and poplar specimens. From longitudinal direction (**Figure S1 to S3**), some cell walls peeled and the surface morphology is irregular. The scalariform perforation plates between vessels were significantly deformed with broken partitions inside as labeled in figures. Another obvious feature of cell wall wrinkling was observed for SE-treated specimens under higher severity factor and acidic condition. These wrinkles were accompanied, especially for acidic specimens, by cracks and collapses for vessel structure, annual rings, and fibers. These broken features were mainly attributed to two factors, the explosive decompression of SE treatment and the drying process, as shown in **Figure 1**. In addition, some droplets appeared on the surface of cell wall after SE treatment, especially for high SE severities. These results could be attributed to the well-known migration or condensation reaction of lignin and the hydrolysis reaction of hemi-cellulose during SE treatment (He et al., 2020; Nader et al., 2021).

3.2 Mass loss and chemical characteristics

Mass loss of SE treated wood specimens is an important feature to evaluate the treatment. As shown in **Figure 5a**, a significant increase in mass loss was observed with severity and in the presence of acid catalysis for the different wood species after SE. For beech specimens, the mass loss ranged from 8.04±0.80 to 16.55±4.89; for poplar, the mass loss was from 2.68±0.51 to 13.45±1.87; for spruce, the mass loss ranged from 6.83±0.58 to 12.91±0.34. This loss of mass is mainly related to the degradation of hemicelluloses according to well-known mechanisms of autohydrolysis or acid hydrolysis and the trends observed were in accordance with

previous study (Gündüz and Aydemir, 2009). A greater increase in mass loss was found for the beech specimens. For the spruce specimens at 180°C-10 min, higher standard deviation was observed compared with other conditions. This result was due to the fact that the specimens were broken into bundles during the pressure release. Even, some part of the specimen was lost especially for the condition of 180°C-15 min. From **Figure 5b**, a decrease in the pH values of the liquid phase was observed for the different species after the SE treatment, especially for the acidic condition. This result could be attributed to the fact that more acidic products were generated during autohydrolysis or acid hydrolysis. For beech and poplar, there was no significant variation among the conditions of 180°C-5 min, 180°C-10 min and 200°C-5 min. While, for spruce, the increase of pH at 200°C-5 min could be due to the short duration of SE treatment. These results also indicated that the temperature, duration and SF should be considered together for different wood species under SE treatment.

Furthermore, the variations of main contents of cell wall components in terms of monomeric sugars (after total hydrolysis) and lignin were analyzed (**Figure 6**). As expected, after glucose, xylose was the dominant monosaccharide in beech and poplar while mannose was the most important in spruce. As stated in previous studies, a decrease in hemicellulose content was obtained especially for higher SF or acidic condition, associated with a relative increase in lignin (He et al., 2020; Ziegler-Devin et al., 2021). However, the result for SE-treated solid wood specimens was different from sawdust and chips. After SE treatment, the slight decrease of hemicellulose for

the specimens was observed for different wood species with higher decrement for the acidic condition. Furthermore, increased xylose was obtained for beech specimen at 200°C-5 min. These results could be attributed to the inhomogeneous distribution of chemical contents among the solid wood specimens after SE treatment. The slight decrease of chemical content also has a positive effect on the mechanical property for SE-treated solid wood specimens.

In order to further investigate the hydrothermal reactions during SE treatment, the FTIR spectra of different wood species were performed as shown in **Figure 7**. The assignments of the mainly FTIR signals are listed in **Table 2**. For beech control specimens, the band at 1235 cm^{-1}, 1505 cm^{-1}, 1650 cm^{-1} and 1738 cm^{-1} were respectively attributed to the C–O stretching vibration, aromatic skeletal vibration plus C=O stretching, absorbed O–H with conjugated C=O and the stretching of C=O in unconjugated ketones, carbonyls and in ester groups. For poplar, the peaks of 1508 cm^{-1},1618 cm^{-1} and 1745 cm^{-1} were assigned to C=C–C aromatic ring stretching vibration, aromatic skeletal vibration of C=O stretching with adsorbed O–H and C=O stretching vibration. For spruce, the bands at 1200 cm^{-1}, 1517 cm^{-1}, 1600 cm^{-1} and 1730 cm^{-1} were attributed to O–H in plane bending vibration, aromatic skeletal vibration, ring stretch vibration related to quinone formation and C=O groups to carboxylation of polysaccharides, respectively (Gonzalez-Peña and Hale, 2011; Zhuang et al., 2020; Rana et al., 2008).

After SE treatment, changes in spectra were observed. The band at ≈ 3362 cm^{-1} attributed to O−H stretching vibration increased and then decreased with increasing

duration of SE treatment for different species. This is due to the fact that the degradation of hemicellulose occurred at the initial stage of the SE treatment and then the drop in pH of the liquid phase led to dehydration reactions resulting in a reduction of hydroxyl content (Wang et al., 2020). The band at 1730 ~ 1745 cm^{-1} assigned to C=O stretching vibration decreased for beech and poplar specimens treated under acidic condition, because of deacetylation reactions involved in the hemicellulose molecules during SE treatment (Tjeerdsma and Militz, 2005).

In addition, the correlations of chemical components and beech lignin main inter-unit linkages contents respectively with ΔE, sphericity and mass loss were obtained for the control and SE-treated specimens as shown in **Figure 8**. High correlation coefficient of 95.45% involved in nonlinear correlation was observed for spruce specimens between lignin content and ΔE parameter while no obvious relationship was found for lignin content of different wood species with ΔE, sphericity and mass loss change rate, respectively (**Figure 8a**). Furthermore, as detected from **Figure 8b**, significant nonlinear correlations of hemicellulose content with ΔE and mass loss rate respectively were obtained for poplar specimens without any correlation coefficient found of hemicellulose content with ΔE and mass loss for the other two species. Moreover, no significant relationship was observed as well between hemicellulose content and sphericity for different wood species. As described in **Figure 8c**, no obvious correlation coefficient was obtained in the relationship of cellulose content with ΔE, sphericity and mass loss change rate, respectively. Better nonlinear correlations of the correlation coefficients ≥ 80% were observed for the

beech lignin main linkages with ΔE, sphericity and mass loss change rate, respectively (**Figure 9**). In this study, SE treatment and the measurements were conducted from solid wood specimens while the composition of lignin was determined in a previous study from beech sawdust (He et al., 2020). As a result, reservations can be made about the correlations made based on the different samples (sawdust and solid wood) and further detailed investigation should be conducted. To some extent, these results provided a great possibility to simulate the morphology, chemical contents, color parameters and mass loss for wood specimens after SE treatment.

3.3 Mechanical and impregnation measurements

Mechanical properties of hydrothermally treated wood are strongly affected by the micro-morphology and chemical composition (Percin et al., 2016). As described in **Figure 10**, the mechanical properties of longitudinal compressive $MOE_{//}$ and $MOR_{//}$ were conducted for treated solid wood specimens compared with the control ones. For the control specimens, higher compressive MOE// and MOR// values were observed for beech and spruce species than that of poplar. This result was due to the different chemical components and anatomical characteristic involved in different wood species.

After SE treatment, for beech and poplar specimens, changes in compressive modulus and strength were obtained depending on the conditions of SE treatment. For beech specimens, higher MOR// and MOE// values were found under the condition of 180°C-15 min compared with the control and other conditions. Moreover, no significant variation was obtained for beech specimens under acidic condition. As

referred to poplar species, no significant change was statistically observed for treated specimens under varied SE conditions based on the Origin significance analysis (at the level of 0.05), except for the acidic-treated ones with the lowest $MOR_{//}$. For spruce, treated specimens were broken easily under higher SFs with no significant variation for the condition of 180°C-5 min as well. As proposed in previous studies, the decrease in mechanical properties observed after hydrothermal treatment is due to the degradation of hemicellulose and the appearance of macro/microcracks during heat treatment. These changes are known to be strongly dependent on wood species, temperature and duration of treatments (Oltean et al., 2007; Poncsak et al., 2006). In this study, SE treatment did not induce a significant decrement on mechanical properties of wood specimens, especially for beech specimens under 180°C-15 min condition and water-treated conditions for poplar and spruce with the comparison of previous research (Kubojima et al., 2000). This result could be attributed to no significant hemicellulose degradation observed for SE-treated solid wood species as shown in **Figure 6**.

The impregnation measurement was then tested for different specimens and the results were shown in **Figure 11**. As the spruce specimens were easy to be broken after SE treatment, the fragments recovered were kept and used only for the impregnation test. For the control specimens, the lowest impregnation ratio was found for beech species and high standard deviations were detected for poplar and spruce species, which were due to nonuniformity of cellular microstructure and the anisotropy among wood species. After SE treatment, for beech and poplar specimens,

higher impregnation ratios were obtained under the condition of 200°C-5 min and 180°C-5 min, respectively with the comparison of other SE conditions. The highest impregnability was observed for spruce species at 180°-15 min condition (**Figure 11a**). These results indicate that the previously mentioned SE-induced morphological and chemical changes have a significant effect on the permeability of solid wood specimens. Interestingly, to some extent, the most effective conditions do not systematically correspond to the most severe conditions. Also, acidic conditions are not conducive to an increase in wood permeability. It was further verified by the fact that no significant relationship between the SF and impregnation ratio for different wood species was observed; for poplar and beech specimens, the peak value of impregnation ratio was at the sphericity of ≈ 0.7 while lower values occurred at higher or lower sphericities; for spruce specimens, negative correlation was found between the sphericity and impregnation ratio (**Figure 11b**). This result can be explained by the decomposition reactions of chemical contents in cell wall components and soft cell wall obtained; on the other hand, low cell wall strength and a higher degree of deformation of the cell lumina, resulted in significant shrinkage of the wood lumina after drying with decreased sphericity values, as indicated by the micro-morphology measurement above. These results indicated that a mild condition (180°C-5 min) was only for poplar solid wood while higher SF condition for beech and spruce solid wood to obtain higher permeability for different wood species.

4. Conclusions

The appearance and permeability of solid wood were significantly changed by SE

treatment. Macro-/micro-cracks were observed with the shrinkage and decreased sphericity for solid wood specimens. Darker tone and higher color parameters of ΔL and ΔE were obtained for higher SF and acidic conditions. No significant decrease in compressive $MOE_{//}$ and $MOR_{//}$ was observed for different wood species except for acidic-treated poplar specimens. The correlations of different factors including SF, chemical content, ΔE, sphericity and mass loss, to some extent, provided a great possibility to simulate the physicochemical and permeable performances for wood specimens after SE treatment. On the other hand, a higher permeability could be obtained under a mild condition of 180°C-5 min for poplar and higher SF condition for beech and spruce species but resulting to significant spruce wood damage.

Thus, SE treatment appears to be an attracting and high-efficient method for solid hardwood treatment to improve its permeability properties. It also provides a positive possibility to further functionally modify natural wood. These high-value solid wood would possess longer period of service and be more widely utilized.

However, SE treatment conditions also induced an increase in multi-scale cracks on the wood structure after the drying process. Thus, an appropriate drying method should be proposed to preserve the morphology of SE-treated specimens.

Acknowledgement

The authors are appreciated for the funding from the Jiangsu Province Postdoctoral Science Foundation [grant number: 2021K474C]. LERMAB is supported by the French National Research Agency through the Laboratory of Excellence ARBRE (ANR-12-LABXARBRE-01) as well. The first author also appreciated for the grand

from the China Scholarship Council (CSC).

References

Akpan E., Wetzel B., Friedrich K., 2021. Eco-friendly and Sustainable Processing of Wood Based Materials. Green Chem, 23, 2198-2232. DOI:10.1039/D0GC04430J.

Balan R., Antczak A., Brethauer S., Zielenkiewicz T., Studer M., 2020. Steam Explosion Pretreatment of Beechwood. Part 1: Comparison of the Enzymatic Hydrolysis of Washed Solids and Whole Pretreatment Slurry at Different Solid Loadings. Energies, 13, 3653. DOI:10.3390/en13143653.

Bekhta P., Mamoňová M., Sedliacik J., Novak I., 2016. Anatomical study of short -term thermomechanically densified alder wood veneer with low moisture content. Eur J Wood Wood Prod, 74, 643-652. DOI:10.1007/s00107-016-1033-2.

Can A., Palanti S., Sivrikaya H., Hazer B., Stefani F., 2019. Physical, biological and chemical characterisation of wood treated with silver nanoparticles. Cellulose, 26, 5075-5084. DOI:10.1007/s10570-019-02416-x.

Donaldson L., Wong K., Mackie K., 1988. Ultrastructure of steam-exploded wood. Wood Sci Technol, 22, 103-114. DOI:10.1007/BF00355846.

Esteves B., Marques A., Domingos I., Pereira H., 2008. Heat-induced colour changes of pine (Pinus pinaster) and eucalypt (Eucalyptus globulus) wood. Wood Sci Technol, 42, 369-384. DOI:10.1007/s00226-007-0157-2.

Gonzalez-Peña M. and Hale, M., 2011. Rapid assessment of physical properties and chemical composition of thermally modified wood by mid-infrared spectroscopy.

Wood Sci Technol, 45, 83-102. DOI: 10.1007/s00226-010-0307-9.

Gündüz G., Aydemir D., 2009. The Influence of mass Loss on the Mechanical Properties of Heat-treated Black Pine Wood. Wood Res-Slovakia, 54, 33-42.

He Q., Ziegler-Devin I., Chrusciel L., Obame S. N., Hong L., Lu X., Brosse N., 2020. Lignin-First Integrated Steam Explosion Process for Green Wood Adhesive Application. ACS Sustain Chem Eng, 8(13), 5380-5392. DOI:10.1021/acssuschemeng.0c01065.

Humar M., Thaler N., Lesar B., 2011. Influence of wood swelling agents on penetration and copper leaching of copper-ethanolamine based wood preservatives, IRG-WP. Stockholm, 11-30556. DOI:10.1007/s00107-009-0317-1.

Kanagaw Y., 1992. Improvement of dryability by local steam explosion for Japanese cedar. Proceedings of 3rd IUFRO Internatinal Wood Drying Conference, 269-276.

Kang C., Kolya H., Jang E., Zhu S., Choi B.-S., 2021. Steam exploded wood cell walls reveals improved gas permeability and sound absorption capability. Appl Acoust, 179, 108049. DOI:10.1016/J.APACOUST.2021.108049.

Kubojima Y., Okano T., Ohta M., 2000. Bending strength and toughness of heat-treated wood. J Wood Sci, 46, 8-15. DOI:10.1007/BF00779547.

Martino D. C., Colodette J. L., Chandra R., Saddler J., 2017. Steam explosion pretreatment used to remove hemicellulose to enhance the production of a eucalyptus organosolv dissolving pulp. Wood Sci Technol, 51(3), 557-569. DOI:10.1007/s00226-016-0889-y.

Minor J. L., Springer E. L., 1993. Improved penetration of pulping reagents into wood. Paper and Timber, 75(4), 241-246.

Monteiro T., Lima J., Neto R. A., Ferreira C., 2020. Importance of Pits in Corymbia Citriodora (Hook.) K.D. Hill & L.A.S. Johnson (Myrtaceae) Wood Permeability. Floresta Ambiente, 28(1), e20200012. https://doi.org/10.1590/2179-8087-FLORAM-2020-0012.

Muzamal M., Gamstedt E. K., Rasmuson A., 2017. Mechanistic study of microstructural deformation and stress in steam-exploded softwood. Wood Sci Technol, 51(3), 447-462. DOI:10.1007/s00226-017-0896-7.

Nader S., Guzman F., Becar R., Segovia C., Fuentealba C., Pereira M., Mauret E., Brosse N., 2021. Lignocellulosic Micro and Nanofibrillated Cellulose Produced by Steam Explosion for Wood Adhesive Formulations. J Renew Mater, 10, 263-271. DOI:10.32604/JRM.2022.017923.

Nicholas D., 1977. Chemical Methods of Improving the Permeability of Wood. 33-46. DOI:10.1021/BK-1977-0043.CH003.

Nimz H. H., 1984. Wood-chemistry, ultrastructure, reactions. Eur J Wood Wood Prod, 42(8), 314-314. DOI:10.1007/BF02608943.

Oltean L., Teischinger A., Hansmann C., 2007. Influence of temperature on cracking and mechanical properties of wood during wood drying - A review. BioResources, 2(4), 789-811. DOI:10.15376/BIORES.2.4.789-811.

Percin O., Peker H., Atilgan A., 2016. The effect of heat treatment on the some physical and mechanical properties of beech (Fagus orientalis lipsky) wood.

Wood Res-Slovakia, 61, 443-456.

Poncsak S., Kocaefe D., Bouazara M., Pichette A., 2006. Effect of high temperature treatment on the mechanical properties of birch (Betula papyrifera). Wood Sci. Technol, 40, 647-663. DOI:10.1007/s00226-006-0082-9.

Pondelak A., Škapin A., Knez N., Knez F., Pazlar T., 2021. Improving the flame retardancy of wood using an eco-friendly mineralisation process. Green Chem, 23, 1130-1135. DOI:10.1039/D0GC03852K.

Qu L., Wang Z., Qian J., He Z., Yi S., 2021. Effects of aluminum sulfate soaking pretreatment on dimensional stability and thermostability of heat-treated wood. Eur J Wood Wood Prod, 79, 1-10. DOI:10.1007/s00107-020-01616-8.

Rana R., Müller G., Naumann A., Polle A., 2008. FTIR spectroscopy in combination with principal component analysis or cluster analysis as a tool to distinguish beech (Fagus sylvatica L.) trees grown at different sites. Holzforschung, 62, 530-538. DOI: 10.1515/HF.2008.104.

Seidel C. -M., Pielhop T., Studer M., Rudolf von Rohr P., 2017. The influence of the explosive decompression in steam-explosion pretreatment on the enzymatic digestibility of different biomasses. Faraday Discuss, 202, 269-280. DOI:10.1039/c7fd00066a.

Sikora A., Kačík F., Gaff M., Vondrová V., Bubenikova T., Kubovský I., 2018. Impact of thermal modification on color and chemical changes of spruce and oak wood. J Wood Sci, 64, 404-416. DOI:10.1007/s10086-018-1721-0.

Simangunsong E., Ziegler-Devin I., Chrusciel L., Girods P., Wistara N., Brosse N.,

2020. Steam Explosion of Beech Wood: Effect of the Particle Size on the Xylans Recovery. Waste Biomass Valori, 11, 625-633. DOI:10.1007/S12649-018-0522-4.

Simpson W. T., 1991. Dry kiln operator's manual Chap.2 Kiln types and features. Forest Products Laboratory, Madison, Wisconsin.

Souza A., Nascimento M., Almeida D., Silva D., Almeida T., Christoforo A., Lahr F. R., 2018. Wood-based composite made of wood waste and epoxy based ink-waste as adhesive: A cleaner production alternative. J Clean Prod, 193, 549-562. DOI: 10.1016/j.jclepro.2018.05.087.

Stamm A., 1932. Effect of Chemical Treatment on Wood Permeability. Ind Eng Chem Res, 24, 51-53. DOI:10.1021/IE50265A014.

Sundqvist B., 2002. Color response of Scots pine (Pinus sylvestris), Norway spruce (Picea abies) and birch (Betula pubescens) subjected to heat treatment in capillary phase. Holz als Roh- und Werkstoff, 60, 106-114. DOI:10.1007/s00107-001-0273-x.

Taghiyari H. R., Majidi R., Arsalan M., Moradiyan A., Militz H., Ntalos G., Papadopoulos A., 2021. Penetration of Different Liquids in Wood-Based Composites: The Effect of Adsorption Energy. Forests, 12(1), 63. DOI: 10.3390/f12010063.

Tanaka T., Avramidis S., Shida S., 2010. A preliminary study on ultrasonic treatment effect on transverse wood permeability. Wood Sci Technol, 12(1), 3-9. DOI:10.4067/S0718-221X2010000100001.

Tarmian A., Tajrishi I. Z., Oladi R., Efhamisisi D., 2020. Treatability of wood for pressure treatment processes: a literature review. Eur J Wood Wood Prod, 78(4), 635-660. DOI:10.1007/s00107-020-01541-w.

Tjeerdsma B., Militz H., 2005. Chemical changes in hydrothermal treated wood: FTIR analysis of combined hydrothermal and dry heat-treated wood. Holz als Roh- und Werkstoff, 63, 102-111. DOI:10.1007/s00107-004-0532-8.

Vroom K. E., 1957. The H Factor: A Means of Expressing Cooking Times and Temperatures as a Single Variable. Pulp Pap Res Inst Can 38, 228-231.

Wang Q., Wu X., Yuan C., Lou Z., Li Y., 2020. Effect of Saturated Steam Heat Treatment on Physical and Chemical Properties of Bamboo. Molecules, 25, 1999. DOI:10.3390/molecules25081999.

Xu H., Taghiyari H. R., Clauson M., Milota M., Morrell J., 2019. Effect of Supercritical Carbon Dioxide Treatment on Gas Permeability of Paulownia Fortunei Heartwood and Sapwood. Wood Fiber Sci, 51, 69-73. DOI:10.22382/WFS-2019-007.

Yorur H., Kayahan K., 2018. Improving Impregnation and Penetration Properties of Refractory Woods Through Cryogenic Treatment. BioResources, 13(1), 1829-1842. DOI:10.15376/BIORES.13.1.1829-1842.

Zelinka S., Passarini L., Matt F., Kirker G., 2019. Corrosiveness of Thermally Modified Wood. Forests, 11(1), 50. DOI:10.3390/f11010050.

Zhang Y., Cai L., 2009. Mechanism for De-aspirating Pits in Subalpine Fir by Steam Explosion Prior to Drying. Dry Technol, 27, 84-88.

DOI:10.1080/07373930802565897.

Zhuang J., Li M., Pu Y., Ragauskas A., Yoo C.G., 2020. Observation of Potential Contaminants in Processed Biomass Using Fourier Transform Infrared Spectroscopy. Applied Sci, 10, 4345. DOI: 10.3390/app10124345.

Ziegler-Devin I., Chrusciel L., Brosse N., 2021. Steam Explosion Pretreatment of Lignocellulosic Biomass: A Mini-Review of Theorical and Experimental Approaches. Front Chem, 9, 705358. DOI: 10.3389/fchem.2021.705358.

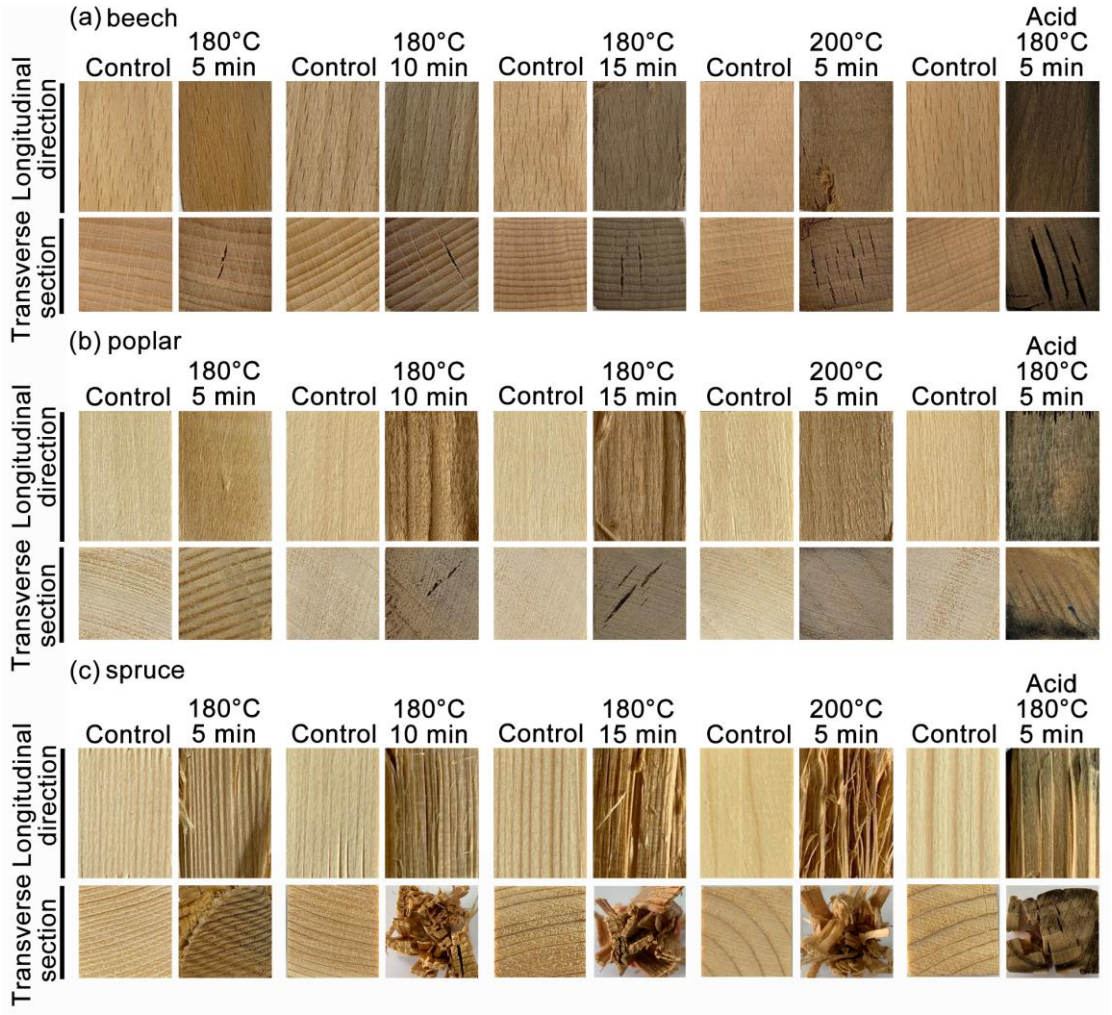

Figure 1. Macro-morphology of SE treated specimens from longitudinal direction and transverse section including (a) beech, (b) poplar and (c) spruce under varied SE conditions.

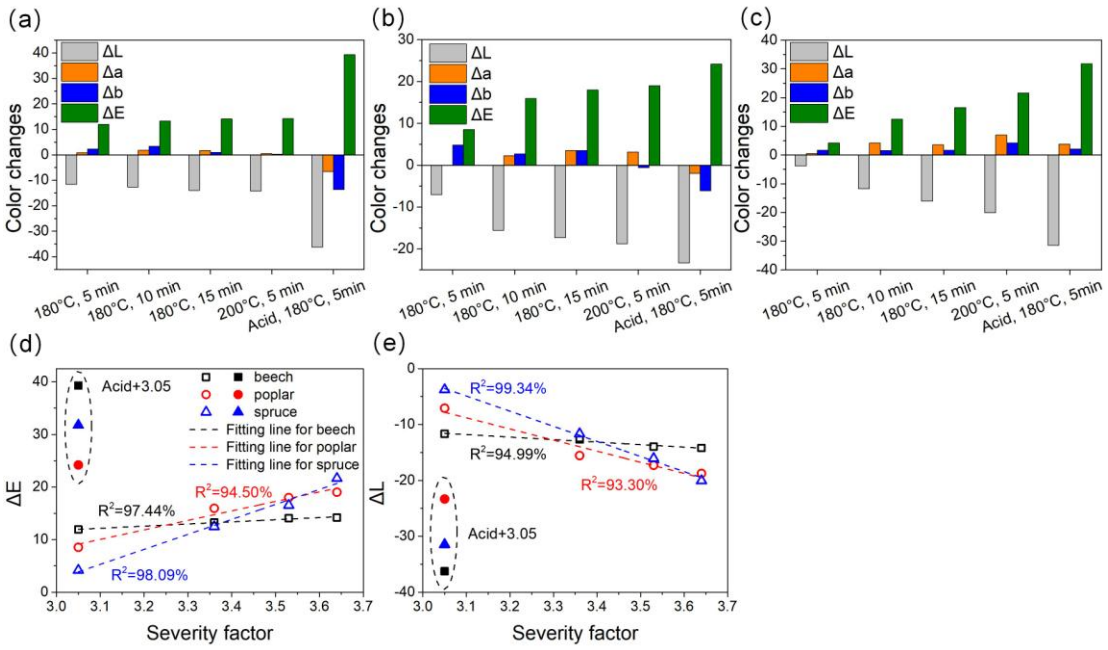

Figure 2. Color difference parameters of SE treated samples including (a) beech, (b) poplar and (c) spruce under varied SE conditions. The correlations of SF with (d) Δ*E* and (e) Δ*L*.

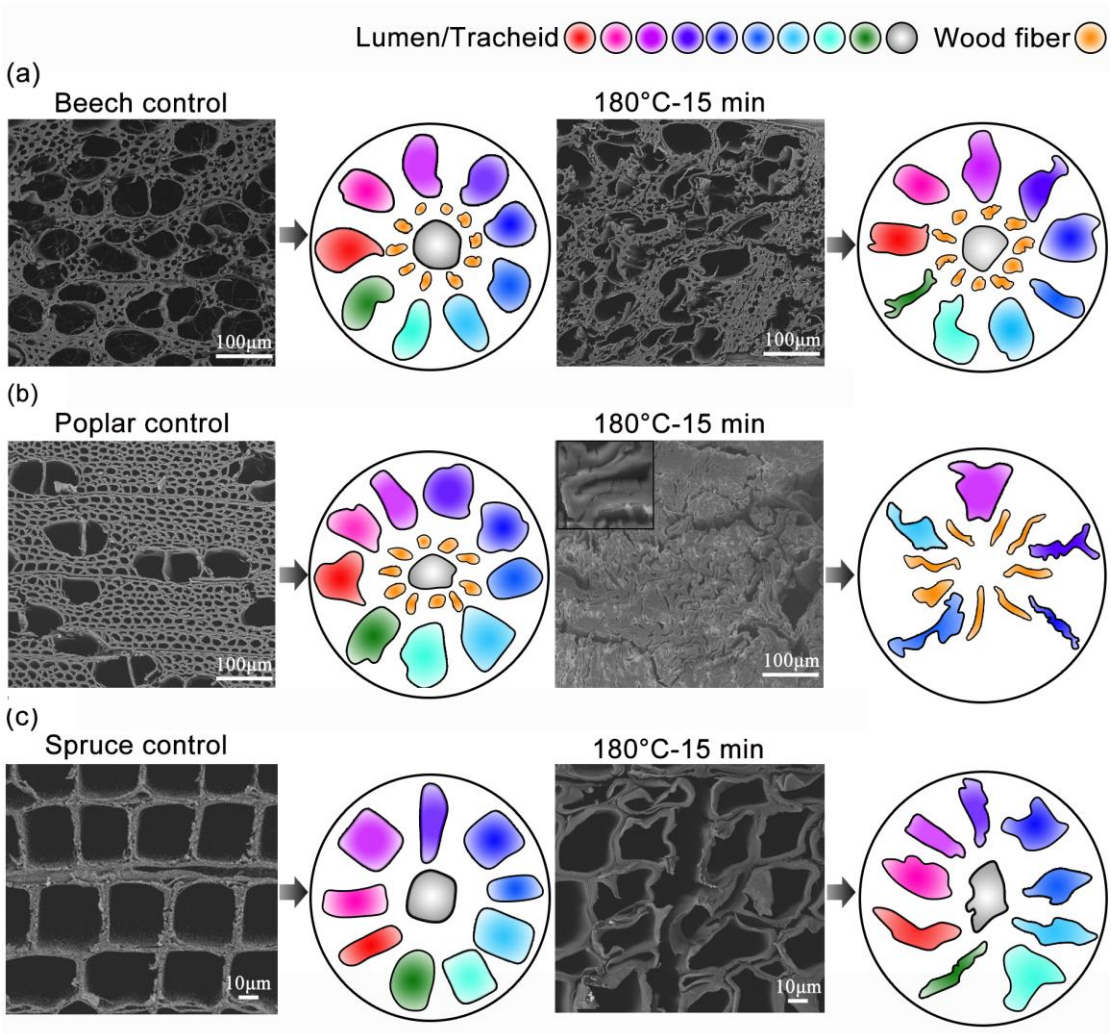

Figure 3. Micro-graphs for (a) beech, (b) poplar and (c) scpruce samples from the cross section under SE condition of 180°C and 15 min with the comparison of control samples. The cellular structures of lumina, wood fiber or tracheids selected from untreated and treated samples, respectively.

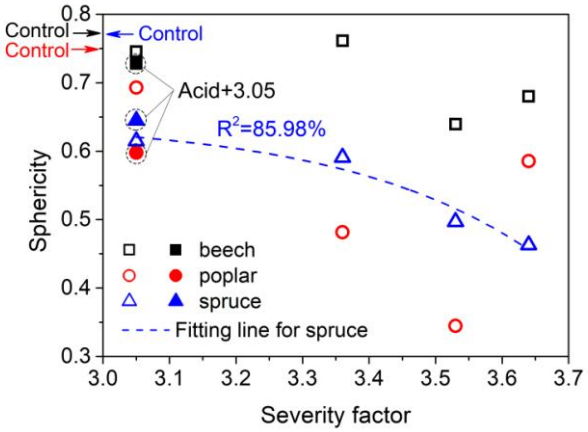

Figure 4. The correlations of varied SFs with the sphericity of cellular structure for different species.

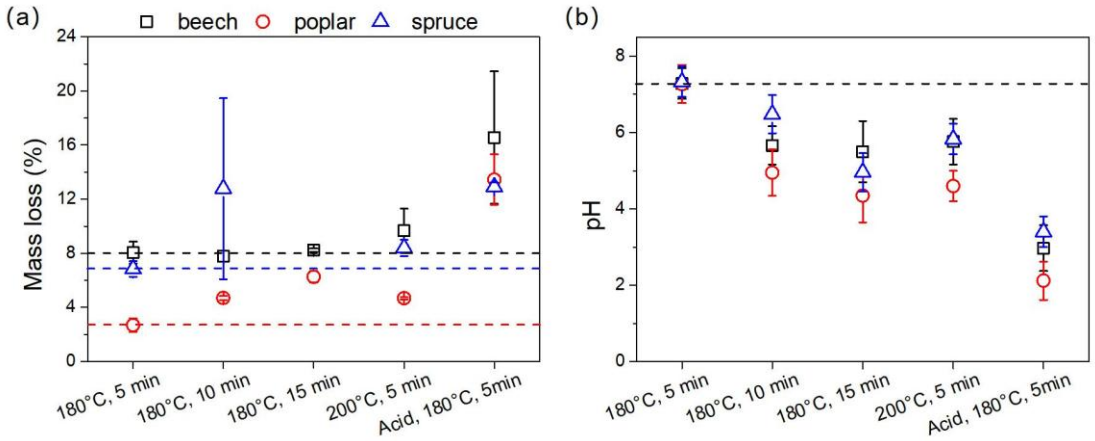

Figure 5. (a) pH value for liquid phase under SE varied conditions for different wood species. (b) Mass loss for SE treated samples under SE varied conditions.

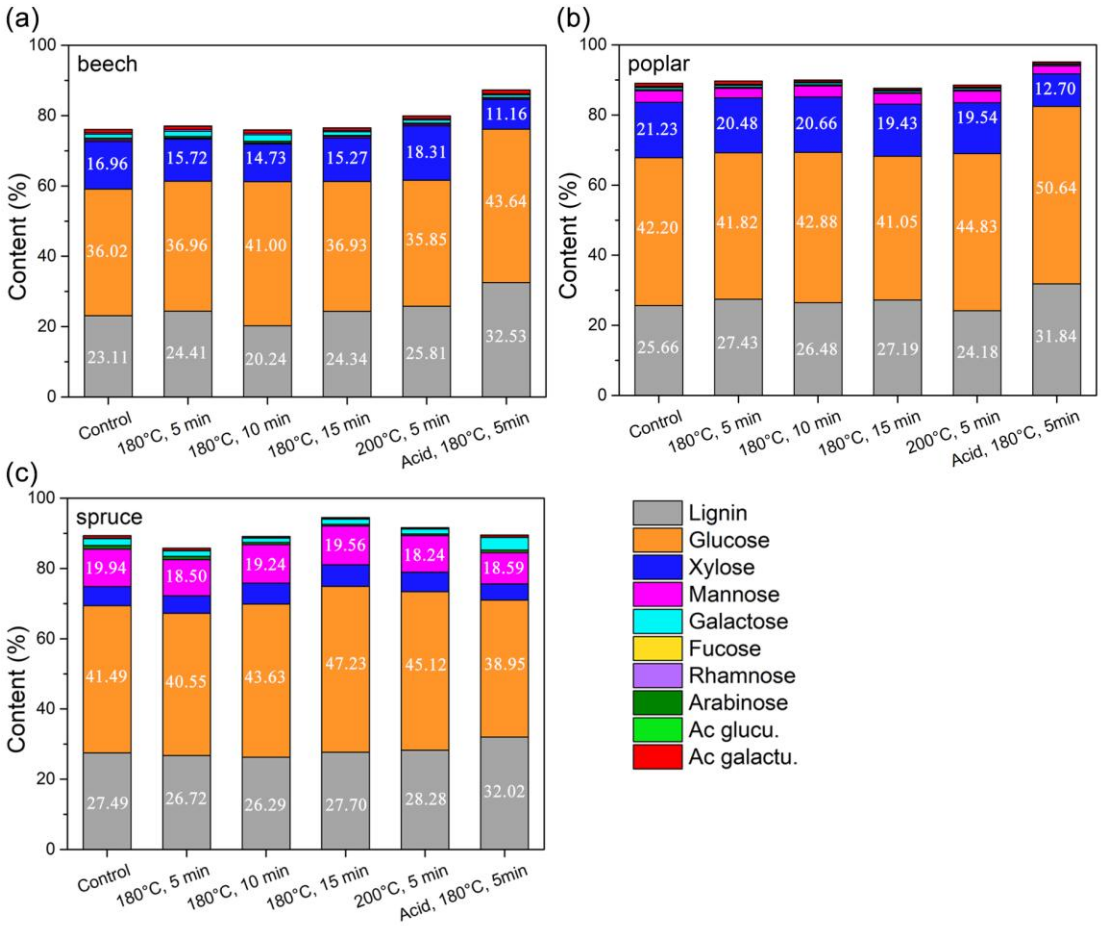

Figure 6. Chemical contents for SE treated samples including (a) beech, (b) poplar and (c) spruce under varied SE conditions. The numbers represented the chemical contents for different species including lignin, cellulose and hemicellulose, respectively.

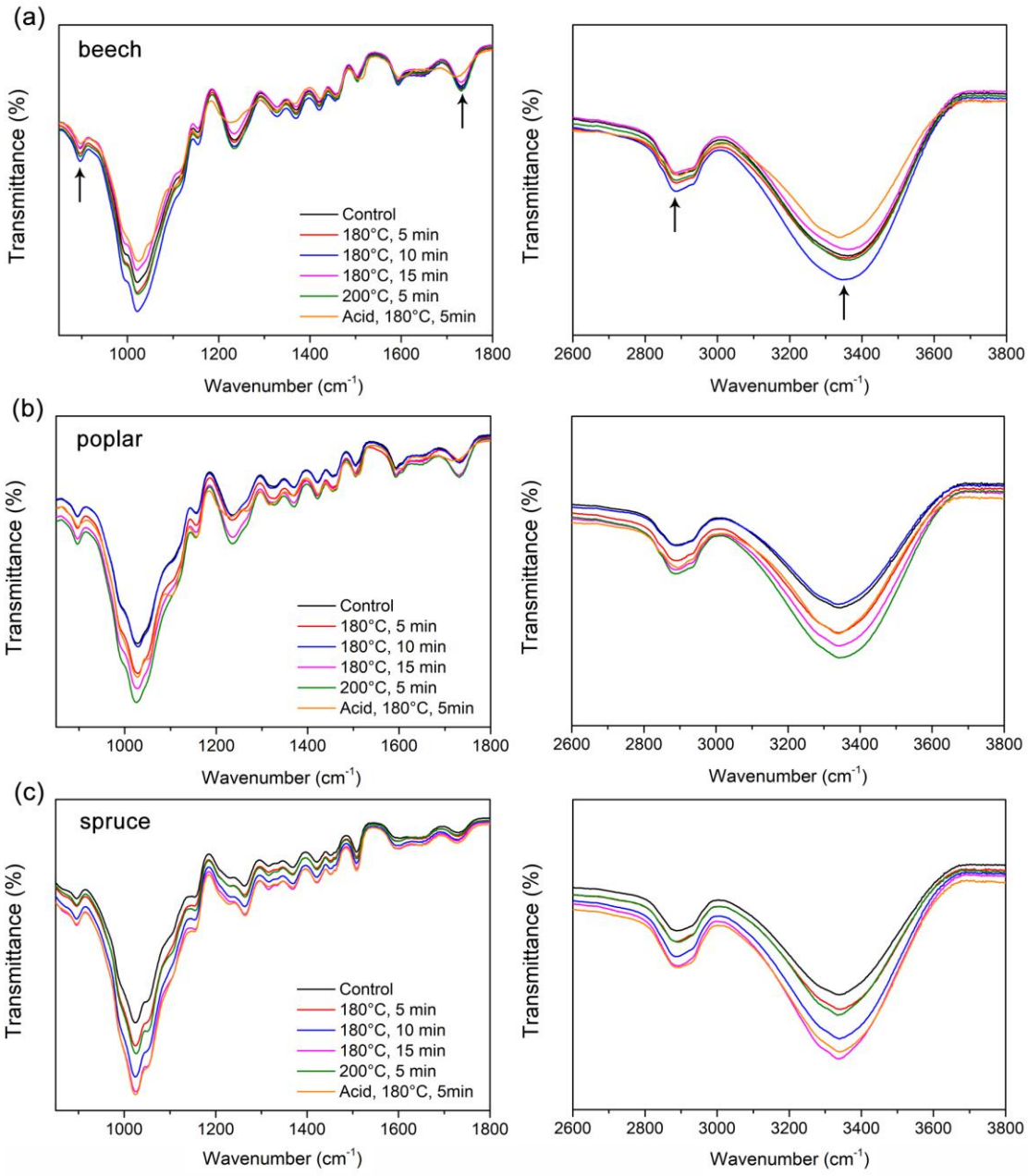

Figure 7. FTIR spectra for SE treated samples including (a) beech, (b) poplar and (c) spruce under varied SE conditions.

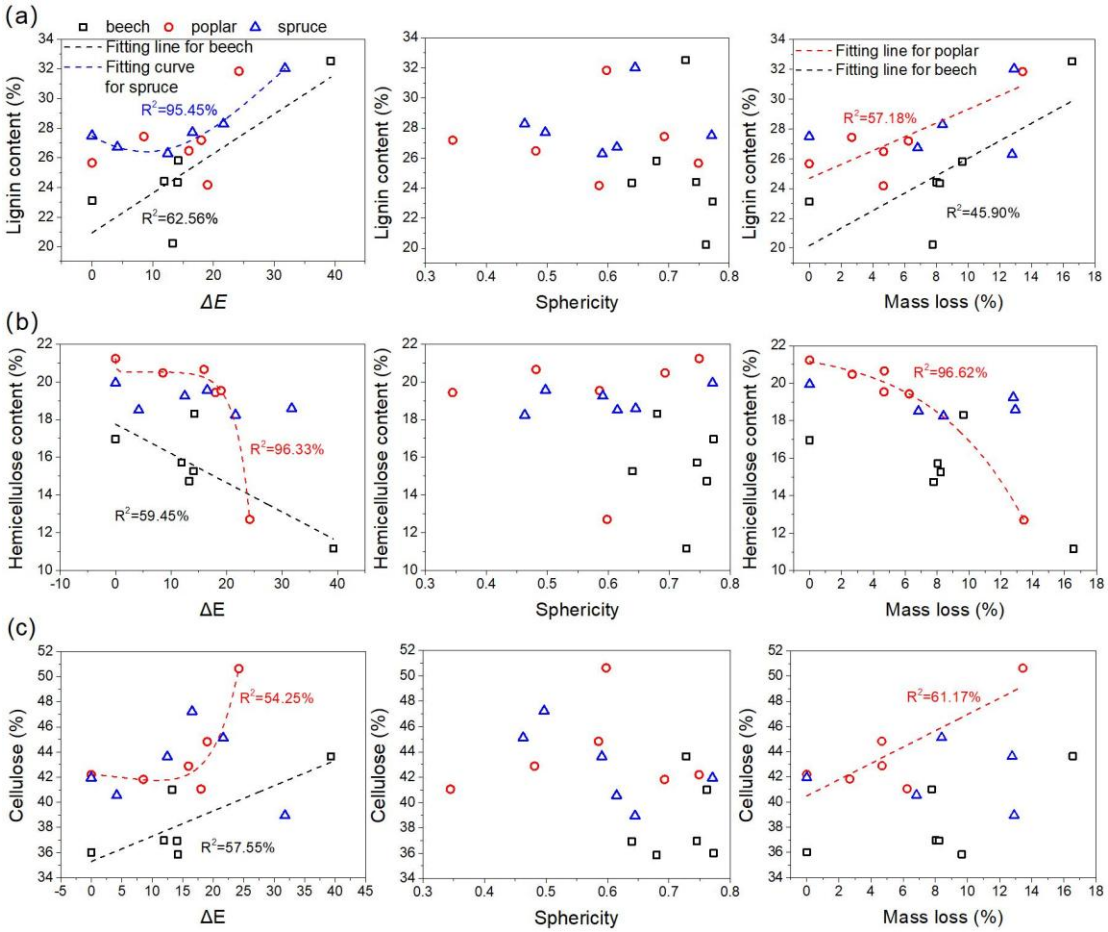

Figure 8. The correlations of (a) lignin, (b) hemicellulose and (c) cellulose contents for the control and SE-treated specimens, respectively with Δ*E*, sphericity and mass loss.

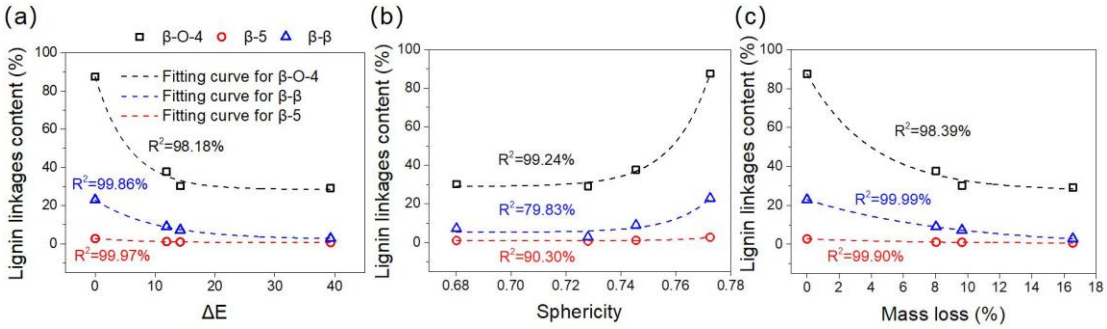

Figure 9. The correlations of the contents of lignin main linkages including β-O-4, β-5 and β-β, respectively with (a) Δ*E*, (b) sphericity and (c) mass loss for the control and SE-treated beech specimens.

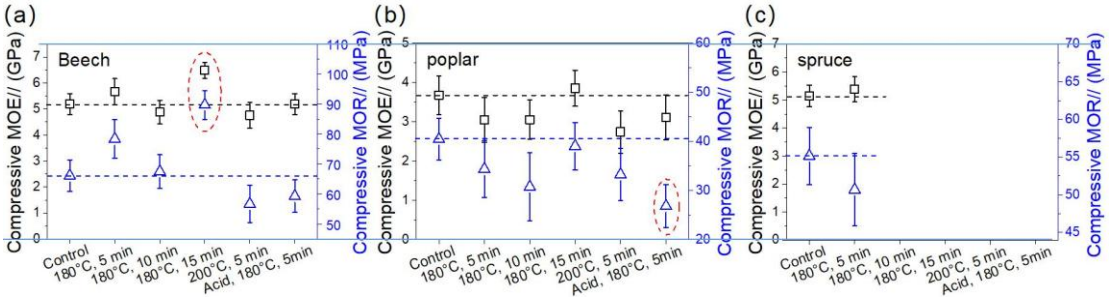

Figure 10. Compressive $MOE_{//}$ and $MOR_{//}$ for SE treated samples including (a) beech, (b) poplar and (c) spruce under varied SE conditions.

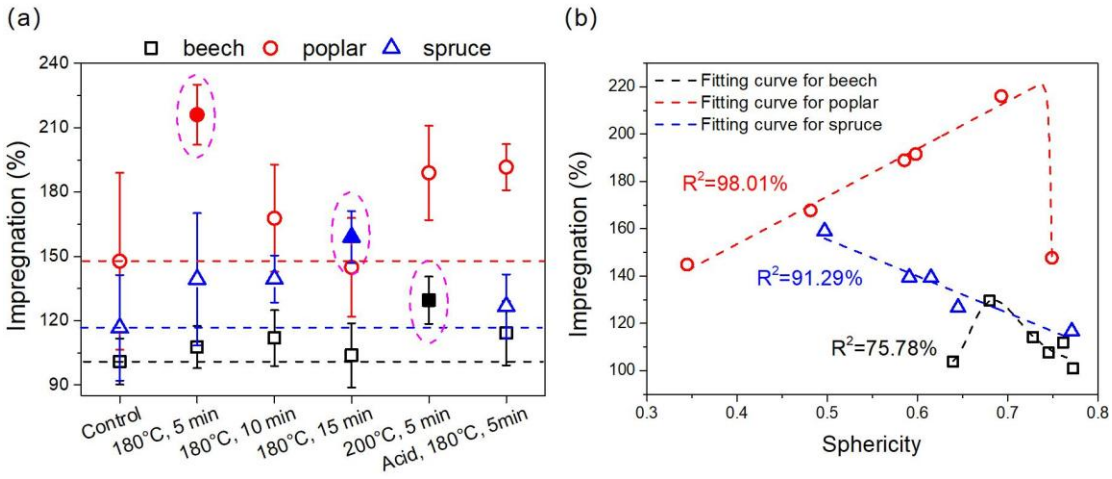

Figure 11. Impregnation ratio of SE treated samples depending on (a) SE conditions and (b) sphericity of cellular structures.

Table 1. Conditions for SE treatment.

Temperature (°C)	Pressure (bar)	Treatment duration (min)	Severity factor	Immersion agent
180	10	5	3.05	distilled water
180	10	5	3.05	1% H_2SO_4
180	10	10	3.36	distilled water
180	10	15	3.53	distilled water
200	16	5	3.64	distilled water

Table 2. FTIR spectra assignments for SE-treated samples.

Band (cm^{-1})	Vibration and assignment
3362	O–H, stretching vibration, intermolecular H bonding (cellulose)
2930	C–H, anti-symmetric stretching, CH_2
2888	C–H, symmetric stretching, CH_2
1745	C=O stretching vibration (poplar)
1738	stretching of C=O in unconjugated ketones, carbonyls and in ester groups (beech)
1730	C=O groups to carboxylation of polysaccharides (spruce)
1650	absorbed O–H with conjugated C=O (beech)
1618	aromatic skeletal vibration of C=O stretching with adsorbed O–H (poplar)
1600	aromatic skeletal vibration, ring stretch vibration related to quinone formation (spruce)
1592	C=C, stretching vibration, aromatic skeleton
1517	aromatic skeletal vibration (spruce)
1508	C=C–C aromatic ring stretching vibration (poplar)
1505	aromatic skeletal vibration plus C=O stretching (beech)
1460	C–H, CH_3 deformation (lignin) and CH_2 bending (xylan)
1424	C–H, CH_2 scissor vibration (cellulose)
1373	C–H, CH_2 bending (cellulose and hemicellulose)
1323	C–H, CH_2 wagging vibration (cellulose)
1235	C–O, stretching vibration (lignin)
1200	O–H in plane bending vibration (spruce)
1153	C–O–C, asymmetric band (cellulose and hemicellulose)
1103	O–H, association band (cellulose and hemicellulose)
1023	C_{aryl}–O ester vibrations, both methoxyl and β–O–4 in guaiacyl units (lignin)
897	C–H, C1 group frequency (cellulose and hemicellulose)